doi.org/10.1002/adsc.202100711
Advanced Synthesis & Catalysis

Carbocatalytic Cascade Synthesis of Polysubstituted Quinolines from Aldehydes and 2-Vinyl Anilines

Mikko K. Mäkelä,[+a] Evgeny Bulatov,[+a] Kiia Malinen,[a] Juulia Talvitie,[a] Martin Nieger,[a] Michele Melchionna,[b] Anna Lenarda,[a] Tao Hu,[c] Tom Wirtanen,[a] and Juho Helaja[a,*]

[a] Department of Chemistry, University of Helsinki, A.I. Virtasen aukio 1, 00014 Helsinki, Finland
E-mail: juho.helaja@helsinki.fi
[b] Department of Chemical and Pharmaceutical Sciences, University of Trieste, Via L. Giorgieri 1, 34127 Trieste, Italy
[c] Research Unit of Sustainable Chemistry, Faculty of Technology, University of Oulu, FI-90014 Oulu, Finland

[+] These authors contributed equally.

Manuscript received: June 8, 2021; Revised manuscript received: July 3, 2021;
Version of record online: July 16, 2021

Supporting information for this article is available on the WWW under https://doi.org/10.1002/adsc.202100711

Abstract: Oxidized active carbon (oAC) catalyses the formation of polysubstituted quinolines from *o*-vinyl anilines and aldehydes. The reaction proceeds in a cascade manner through condensation, electrocyclization and dehydrogenation, and gives access to a wide range of quinolines with alkyl and/or aryl substituents as demonstrated with 40 examples. The metal-free catalytic procedure allows a heterogeneous protocol for the synthesis of various polysubstituted quinolines. The mechanistic studies imply that both the acid and quinoidic groups in oAC are integral for the catalytic manifold.

Keywords: Carbocatalysis; Quinoline; Oxidative Dehydrogenation; Electrocyclization

Quinoline synthesis is one of the most traditional methods to benchmark novel synthetic methodologies against both classical and more modern approaches. Consequently, a wide range of synthetic methodologies for substituted quinolines have been documented.[1] Amongst several different strategies, reacting anilines with various annulation partners (e.g., alkynes, aldehydes, α,β-unsaturated, and 1,3-dicarbonyl compounds) has been a particularly popular strategy due to the easy access to substrates that can be converted to a wide range of quinoline derivatives.[2]

Herein, we report the synthesis of polysubstituted quinolines from *o*-vinyl anilines and aldehydes using a *carbocatalyst*, an oxidized active carbon, as a promoter. Carbocatalysis is well known to the catalysis and industrial chemistry communities, where it continues to attract attention,[3,4] but it is perhaps less familiar among organic chemists. Nevertheless, carbocatalysts such as active carbons (ACs), graphene oxides (GOs),[5] and carbon nanotubes (CNTs) can mediate various types of organic conversions such as additions, substitutions, (de)hydrogenations and redox reactions.[6] In particular, the emergence of GO vitalized the field, initially appearing as carbocatalyst in Bielawski's seminal benzyl alcohol oxidation.[7] Later on, his and other laboratories have reported that GO could catalyse a variety of synthetic reactions, including oxidations of thiols and sulfides,[8] aza-Michael additions,[9] aldol reactions,[10] C–H activations/coupling reactions,[11–13] and Friedel-Crafts alkylations.[14] Lately, Bielawski reported asphaltene oxide as a soluble variant of GO.[15] Before these developments, Hayashi's group disclosed that activated

carbons (AC) can catalyse oxidative dehydrogenative (ODH) aromatization of N-heterocycles.[16] These type of carbocatalytic reactions have been later utilized also by others.[17] In addition, we have previously reported that oxidized activated carbon (oAC) can catalyse ODH homocouplings of benzofused heterocycles as well as dehydrogenations of N-heterocycles.[18] In most cases, the catalytic activity of carbon materials are correlated to the distribution of O-containing functional groups (*e.g.*, –COOH, C=O) on their surface, and, interestingly, their abundance can be fine-tuned by different oxidative treatments. The catalytic action that these grafted groups project to different substrates follow the same logic as in traditional organic synthesis. For example, carboxylic acids promote acid catalysed conversions,[19,20] while quinoidic sites have been correlated to catalytic activity in dehydrogenation reactions.[3,21]

As quinoline derivatives are a ubiquitous class of heterocycles among biologically active molecules, we reasoned that heterogeneous carbocatalytic access to different quinolines would be valuable. We focused our attention on the three-step cascade reaction between *o*-vinyl anilines and aldehydes (Figure 1) where the first step is dehydrative formation of an imine intermediate, which thermally electrocyclizes to a dihydrointermediate, that is finally oxidized to a quinoline. Plausibly, the carbocatalyst could participate in each of the three steps: i) either acids or the graphitic surface could assist in the imine formation,[22] ii) the latter could stabilize the reaction intermediates as well,[23,24] iii) and quinoidic groups could assist in the final oxidation of the dihydrointermediate to the target molecule.[25] As the annulative electrocyclization, which is the most probable rate-determining step (RDS) in this cascade, is known to typically require harsh conditions such as high temperatures (155–200 °C)[26] or strong acid catalysis (*p*-TsOH, CF_3CO_2H, TfOH)[27] there is a strong urge to develop milder methods so that more sensitive derivatives (e.g., alkynes and furans) can be accessed with this synthetic strategy. Moreover, both the thermal and acid catalysis lead to the concomitant formation of *N*-aryl amine side products which somewhat lower the yields (Figure 1). In the absence of a suitable oxidant, *N*-aryl amines are formed when imines oxidize the dihydroquinoline intermediates to quinolines (Figure 1).

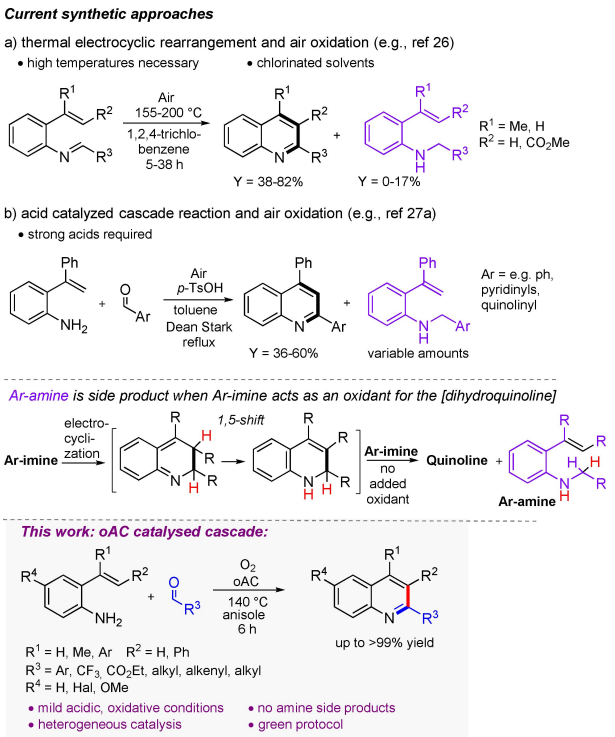

Figure 1. Electrocyclic synthesis of quinolines from *o*-vinyl anilines and aldehydes.

Recently, we demonstrated that a thermal treatment (450 °C) of AC under air is a simple and relatively mild yet effective oxidative protocol for producing a catalytically active carbon material with a moderate oxygen content and a high surface area for oxidative aryl couplings.[23] Using this material as catalyst (oAC-air(450)), we started to optimize the yield of the reaction between 2-isopropenylaniline **1a** and benzaldehyde **2a** (Table 1 and Table S8). The screening of the reaction conditions revealed that, in addition to the desired quinoline **4a**, the reaction can also afford intermediate imine **3a**, secondary amine **3a'**, and uncharacterized oxidized side products. The best result of 85% was obtained with 1.15 equiv. of **1a** under oxygen atmosphere using 100 mg of carbocatalyst per mmol of **1a** (Table 1, entry 1). The oxygen atmosphere was essential since the yields dropped to 78% and 62% under air and argon atmospheres, respectively, due to the formation of secondary amine **3a'** (Entries 2, 3 and Mechanistic Studies in SI). Similarly, **3a'** evolved at 154 °C even though the yield of **4a** increased slightly to 87% (Entry 4). This can be attributed to the combined effect of the increased rate of the thermal cyclization[26] and the reduced concentration of the dissolved oxygen. Expectedly, lowering the temperature to 130 °C or the reaction time to 3 h resulted in lower yields of 67% and 69%, respectively (Entries 5, 6). Prolonged reaction time caused partial oxidation of the 4-Me group to aldehyde (See Mechanistic studies in SI). Lowering the catalyst loading to 50 mg/mmol also diminished the yield slightly to 82% (Entry 7). Interestingly, with a higher catalyst loading of 200 mg/mmol only 72% of **4a** was received (Entry 8). This was probably due to the absorption of **1a** on the carbon material (See discussion of Figure 2b). The use of preformed imine **3a** as a starting material under the optimal conditions afforded a lower yield of 72% (Entry 9). Using *o*-xylene as a solvent afforded slightly higher yield (Entry 10), yet, the choice of anisole as

Table 1. Optimization of the reaction conditions.[a]

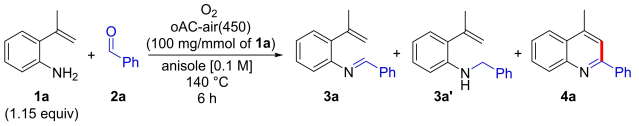

entry	change from the standard conditions	yield (%)[b] 3 a (3a')	4 a
1	none	4	85 (82)[c]
2	air atmosphere	3 (12)[d]	78
3	Ar atmosphere	0 (36)[d]	62
4	temp = 154 °C (reflux)	0 (6)[d]	87
5	temp = 130 °C	15	67
6	time = 3 h	17	69
7	50 mg/mmol catalyst load	12	82
8	200 mg/mmol catalyst load	1	72
9	starting from **3 a**	2	72
10	*o*-xylene as a solvent	5	89
11	10 mol% pyridine as additive	6	79
12	10 mol% 4-fluorobenzoic acid as additive	4 (7)[d]	84
13	no catalyst	19	2
14	starting from **3 a**, no catalyst	73	15
15	pristine AC as catalyst	67	20
16	oAC-air(425) as catalyst	9	77
17	oAC-air(475) as catalyst	6	87
18	GO as catalyst[e]	18	53
19	oCNT as catalyst[f]	27	68
20	1 mmol scale, 130 mg/mmol catalyst load	4	83 (80)[c]

[a] Reactions were performed on a 0.15 mmol scale.
[b] Yields were determined by NMR analysis using 1,3,5-trimethoxybenzene as an internal standard.
[c] Isolated yield.
[d] NMR yield of *N*-benzyl-2-isopropenylaniline (**3a'**) side product (details on formation of **3a'** are presented in the SI).
[e] 2-4 layer graphene oxide produced by a modified Hummer's method.
[f] Oxidized multi-wall carbon nanotubes prepared according to ref. [29].

solvent is justified by sustainability aspects.[28] The acidity of the catalyst is expected to have a role in the cascade reaction (Entries 11, 12). Therefore, two experiments were run in presence of 10% pyridine and 10% 4-fluorobenzoic acid dopants. While pyridine slightly lowered the yield to 79%, the addition of the acid additive afforded it to 84%, increasing the formation of the amine **3a'** side product as well. This indicates that decreasing the acidity slows down the reactivity, while increasing acidity lowers the selectivity.

In the absence of catalyst, only a 2% and 15% **4 a** was received from either **1 a** and **2 a** or **3 a**, respectively (Entries 13, 14). The degree of oxidation of AC was found crucial for the catalytic activity. The pristine AC or the catalyst prepared at 425 °C afforded lower yields

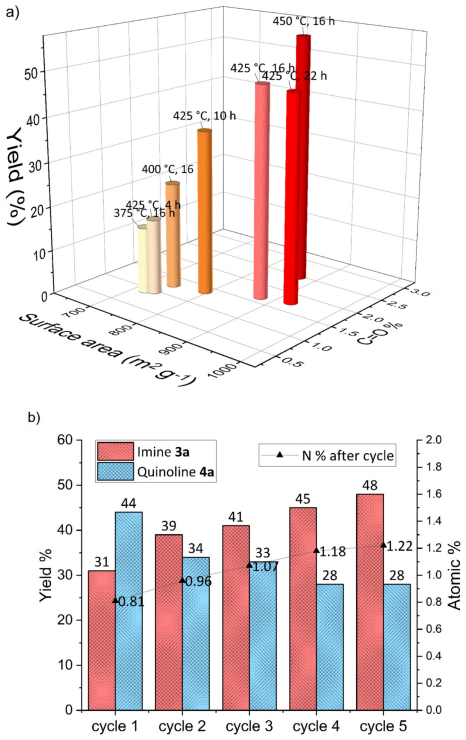

Figure 2. a) Catalytic activities against XPS analyzed C=O content and BET defined surface area of various oAC materials obtained by different oxidative treatments, b) Recycling tests for **1 a** + **2 a** to quinoline **4 a** conversion with oAC-air(425). Reaction conditions: catalyst loading 224 mg/mmol, 110 °C, 4 h. Blue and red bars represent NMR yields of **4 a** and **3 a** accordingly. Triangles display the sum of pyridinic and pyrrolic atomic % content on the carbon material after each related cycle obtained from XPS analysis.

of 20% and 77% of **4 a**, respectively (Entries 15, 16). Using oAC oxidized at 475 °C afforded a slightly higher yield of 87% (Entry 17), however, the results were not as reproducible, and the catalyst preparation was in general less efficient (see SI for further details). Therefore we chose to use oAC-air(450) as the carbocatalyst (for further details, see SI). Furthermore, the other commonly employed oxidized carbon materials GO and oCNTs delivered slightly lower yields of 53% and 68%, respectively (Entries 18, 19). The reaction performed at 1 mmol scale using 150 mg of catalyst afforded **4 a** in 80% isolated yield after 6 h demonstrating the scalability of the studied reaction (Entry 20).

With the optimized reaction conditions in hand, we explored the scope and the limitations of the cascade synthesis. The reaction between 2-isopropenylaniline **1 a** and aldehydes **2 a-i** afforded the corresponding 4-methylquinolines **4 a–i** in fair to good yields (Scheme 1), revealing tolerance to both electron deficient and electron rich aldehydes.

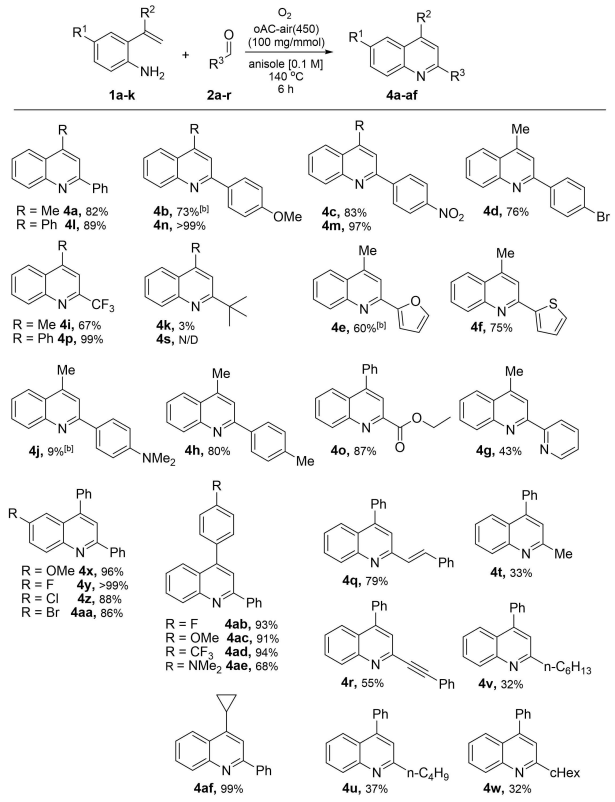

[a] Isolated yields.

[b] Using the catalyst load 224 mg/mmol, 130 °C, 4 h.

Scheme 1. Scope of 4-substituted quinolines.[a]

Pleasantly, 4-phenylquinolines **4 l–s** could be obtained from 2-(1-phenylvinyl)aniline **1 b** in generally higher yields than the methyl derivatives. The reason for the higher yields of the 4-phenyl over 4-Me derivatives is presumably related to the slow oxidation of the methyl to an aldehyde group (see SI: Table S9 and Mechanistic Studies). Furthermore, with 4-phenyls, it was possible to introduce more challenging substituents at the 2-position, including aliphatic groups. These derivatives **(4 t–w)** were isolated in 32–37% yields. This demonstrates that the mildly acidic oAC catalysis is more convenient than the homogeneous acid catalysis and thermal reaction as both were found unsuitable for these type of substrates due to competing aldol condensations.[26] Furthermore, anilines **1 c-j** produced quinolines with both EDG and EWGs at the 6-position (**4 x–aa**) and in *para*-substituted phenyls at 4-position (**4 ab–ae**). Interestingly, despite the tendency of the cyclopropyl rings to undergo ring opening in radical reactions, 4-cyclopropylquinoline **4 af** was obtained from **1 k** in quantitative yield. The presence of dimethylamino and *tert*-butyl groups appeared to be detrimental for the yield of quinolines **4 j,k,s** and **4 ae**.

The scope of the cascade reaction was further expanded to 4-H quinolines starting from 2-styrylaniline **1 l**. Significantly lower activity of these substrates was observed and it was therefore necessary to tune the reaction conditions by extending the reaction time from 6 to 40 h and increasing the loading of the catalyst to 800 mg/mmol (Table S9). Nonetheless, the corresponding 3-phenylquinolines **4 ag–al** could be obtained in fair to good yields (Scheme 2). However, 18% yield of 2-phenylquinoline **4 am** was received when 2-vinylaniline **2 m** was used as a substrate under the same conditions.

The recycling experiments show clearly that oAC operates in a catalytic manner even though the catalyst efficiency drops approximately by 15% after five reaction cycles (Figure 2, Table S10). We analysed the carbons with X-ray photoelectron spectroscopy (XPS), so to quantitatively define the chemical state of the elements on the carbon surface. The observed decay of catalytic activity is associated with an increasing formation of pyridinic and pyrrolic functional groups in the oAC material (Figure 1, Table S5), which can be ascribed to the physi- and chemisorption of aniline on oAC (See Mechanistic Studies in SI). We speculate that these functional groups have similar detrimental effects on the catalytic activity than the pyridine additives (Table 1).

The XPS analysis of various tested catalytic materials indicate that the yields of the cascade reactions correlate with the linear regression of C=O and C–OH content (Tables S1 and S3, Figure S1). These groups can form the quinone/hydroquinone redox pair that is relevant for the quinoidic dehydrogenations of the cyclized dihydrointermediate. The relevance of functional groups distribution on oAC for catalysis was further supported by the catalytic activity tests run with catalysts with selectively protected C=O, COOH, and C–OH groups (Table S2). The results indicated a significant decrease in the reaction yield for the catalyst with protected C=O groups, whereas protection of the other groups did not induce considerable changes. Figure 2a, additionally, evidences the

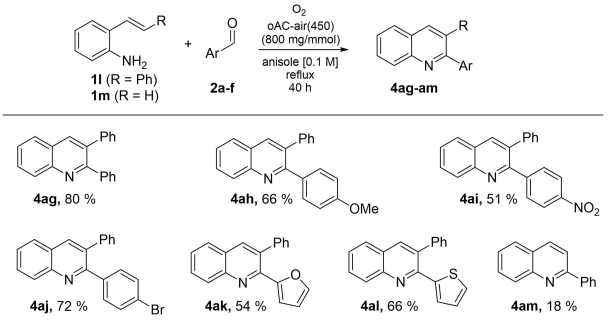

[a] Isolated yields.

Scheme 2. Scope of 4-H-quinolines.[a]

correlation between yield, Brunauer-Emmett-Teller (BET) surface area and % C=O, providing additional proof of the criticality of carbonylic functionalities to the catalytic process. Inductively coupled plasma mass spectrometry (ICP-MS) analysis of oAC proved the metal-free nature of catalysis, as the most transition metals are present solely in traces (Table S7), with the only exception of iron, which abundance is slightly higher (737 ppm). Yet, using Fe-doped carbon as catalyst delivered only reduced yields of **4 a**: spiking the catalyst with additional 1 and 5 wt% of iron lowered the reaction yields to 71% and 65%, respectively (SI), proving that the added iron has no beneficial effect on the catalytic process.

In order to get further insight on the mechanism of the cascade reactions, kinetic experiments were undertaken with various electron-donating groups (EDG) and electron-withdrawing groups (EWG) substituted anilines and aryl aldehydes: the results are presented in Figure 3 and S2–8. In all the cases, fast and reversible formation of intermediate imines is observed, whereas their oxidative cyclization to quinoline is irreversible in the overall cascade process. While affecting the equilibrium between the starting compounds and the intermediate imine, the electronic properties of substituents R^1 on the aniline ring have no significant effect on the overall reaction rate (Figure 3a). The variation of R^3 on the aldehyde has an observable effect on the rate (Figure 3c) as the electron withdrawing NO_2 group slightly increases and the electron donating OMe reduces the rate. On the contrary, R^2 in *para*-position of 4-phenyl ring has a pronounced effect on the quinoline formation rate, with electron donating –OMe group affording one order higher reaction rate compared to electron withdrawing $–CF_3$ group (Figure 3b).

For gaining theoretical insight of possible mechanistic routes, we performed computational studies at DFT level (pw6b95d3/def2-tzvp//pbe0-D3bj/def2-svp (CPCM anisole)). First, we inspected the initial cyclization step of *N*-2-(isopropenyl)phenyl-1-arylmethanimines **3 a**–**3 c** (Figure S9). On the one hand, the fairly high computed oxidation potentials of the studied imine intermediates (> 1.3 V, vs. SCE) exclude the formation of radical cation intermediates, that potentially could have low energy barriers for cyclizations, since our previous studies insist that solely the substrates with oxidation potentials lower than + 1.0 V (vs. SCE in MeCN) can be oxidized by oAC (Figure S9).[29,30] On the other hand, the calculated barriers for protonated imines suggest that acid catalysis could lower the cyclization energy barriers by 7–10 kcal/mol. However, the used carbon materials contain relatively low amount of carboxylic acids, and they in turn are too feeble acids to protonate the studied imines. Hence, thermal electrocyclization can be reasoned to represent the most probable pathway. The used experimental conditions (Table 1) would, in fact, allow crossing the calculated cyclization transition state free energy barriers of 26, 30 and 31 kcal/mol for **3 a**, **3 b** and **3 c**, respectively.

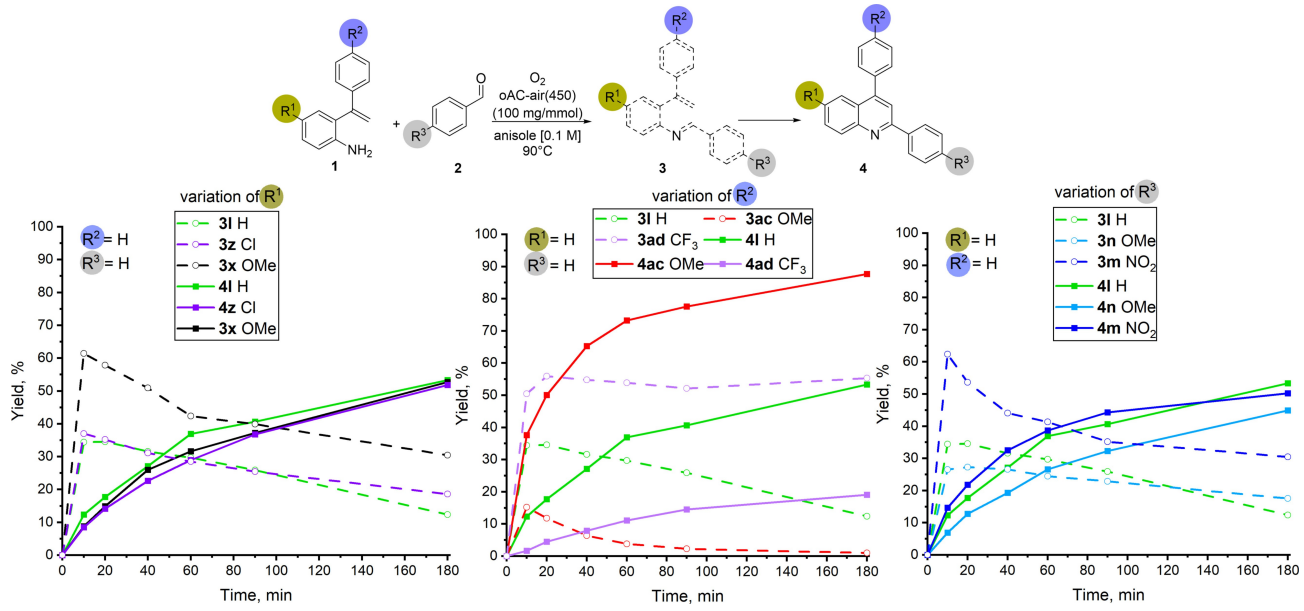

Figure 3. Monitoring of progress of the reactions (^{1}H NMR) with substrates **1** and **2** by varying EWG/EDG substituent at a) R^1, b) R^2 and c) R^3 positions. Solid lines with filled squares represent yields of quinolines, and dashed lines with empty circles represent yields of intermediate imines. Reactions were performed under standard conditions, except 0.1 mmol scale, 90 °C, and 5% aniline excess.

At the second stage, relying on the thermal electrocyclization mechanism, we looked for a theoretical explanation for the measured kinetics in Figure 3, and calculated full energy profiles from imines **3 l**, **3 ac**, **3 ad**, **3 n** and **3 m**, to corresponding quinolines **4 l**, **4 ac**, **4 ad**, **4 n** and **4 m** using *o*-benzoquinone (*o*BQ) as quinoidic dehydrogenation model probe for the catalyst material (Figure 4). The calculated cyclization barriers, 28.0–29.7 kcal/mol correlate qualitatively well with the observed quinoline formation rates. Electron donating OMe group at R^2 position lowers and at R^3 position raises the barrier ca. 1 kcal/mol. Meanwhile, electron-withdrawing groups (CF_3 and NO_2) at these positions have similar effects into opposite directions. Remarkably, [1,5] H-shifts from 2,3-dihydroquinoline to 1,2-dihydroquinoline derivatives reported earlier for thermal reactions (> 155 °C)[26] form another high (29.1–29.8 kcal/mol) energy barrier for the imine series. This might explain why under the used catalytic conditions we did not observe any formation of 1,2-dihydroquinolines. In this scenario, the carbocatalyst is not involved in the cyclization step but it would rather dehydrogenate the cyclized 2,3-dihydroquinoline derivatives to quinolines.

The calculation of dehydrogenation barriers of dihydrointermediates **4H$_2$l**, **4 H$_2$ac**, **4 H$_2$ad**, **4 H$_2$n** and **4 H$_2$m** with *o*BQ as model quinone resulted in low values, 11.5-12.5 kcal/mol, for hydrogen abstraction at C2-position (Figure 4). After this step, the reaction pathway is highly exergonic. Analogous calculation for **4H$_2$l** with a larger model quinone, phenanthrenequinone, resulted in somewhat higher barrier 19.9 kcal/mol for the first dehydrogenation (SI), although still rather low compared to the cyclization or [1,5] H-shift barriers. Overall, the calculations support the mechanistic view that implies that, in the presence of a quinoidic oxidant, the rate-limiting step would be thermal electrocyclization. Finally, a radical trapping test was performed using the standard reaction in the presence of the free radical TEMPO additive (SI). The

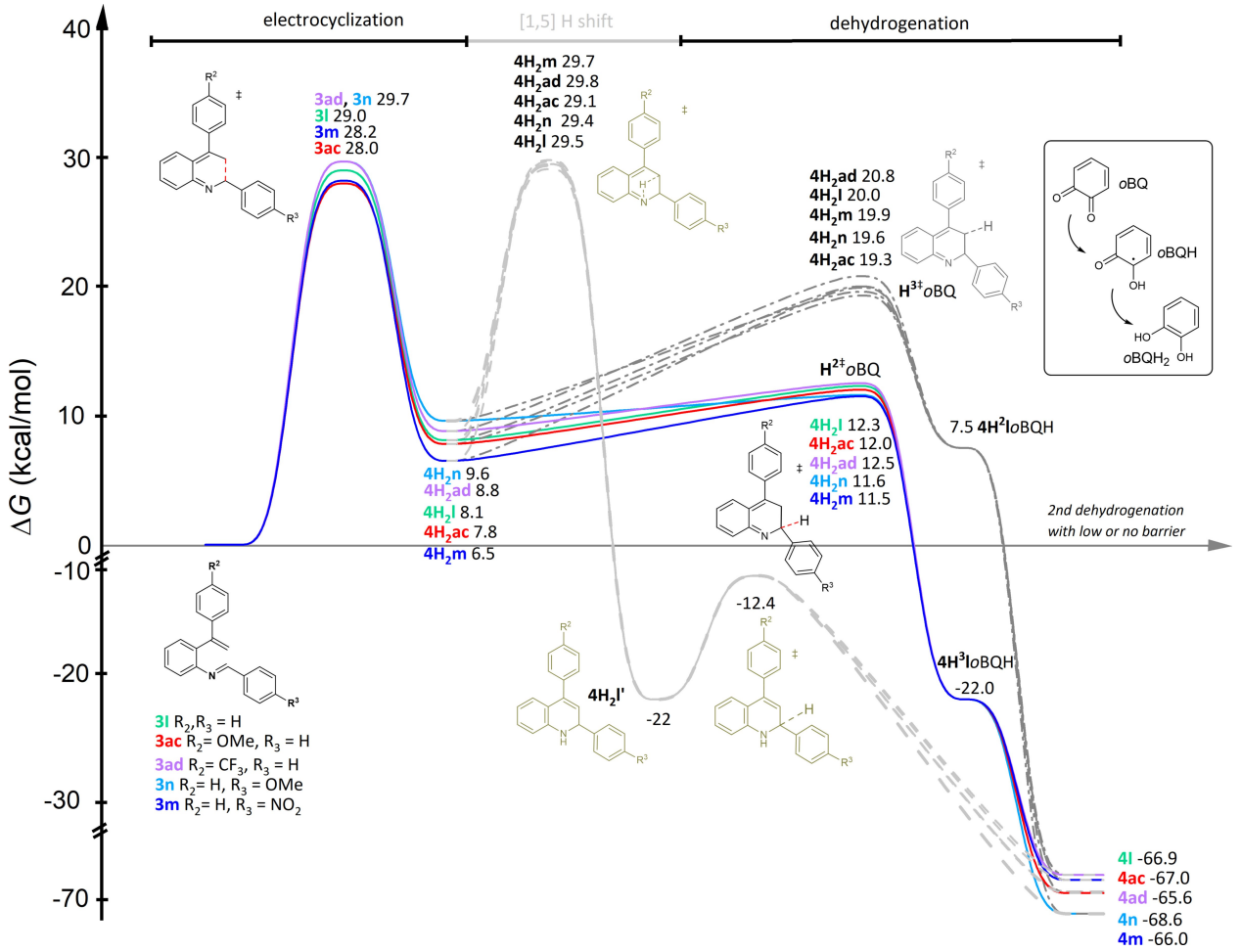

Figure 4. Free energy profiles for 2,4-aryl quinoline reactions from the corresponding imines calculated with method pw6b95/def2-tzvp//pbe0/def2-svp empirical dispersion = gd3bj (CPCM anisole). Dehydrogenation steps are calculated by using *o*-benzoquinone (*o*BQ) as a quinoidic model oxidant.

yield of quinoline **4a** was reduced from 85% to 12% by the addition of two equivalents of TEMPO, indicating involvement of radical species in the reaction mechanism. Based on the combined data of experimental and computational studies, we propose the following cascade mechanism (Scheme 3): the reversible formation of imine **3a** is followed by reversible thermal electrocyclization. The carbocatalysts then perturbs this equilibrium by irreversibly oxidizing the cyclized dihydrointermediate to the final quinoline **4a**. The reduced form of the carbocatalyst is then oxidized by dioxygen and generates water (or hydrogen peroxide) as a by-product.

In summary, we have devised a carbocatalyzed cascade reaction protocol to access quinolines from *o*-vinyl anilines and aldehydes. A thermal procedure was developed to oxidize AC to catalytically active oAC capable to act both as Brønsted acid catalyst in imine formation and quinoidic dehydrogenation catalyst for dihydroquinoline aromatization to deliver polysubstituted quinolines without the formation of reduced amine side products.

Experimental Section

Preparation of oxidized active carbon (oAC). Activated charcoal (16.9 g) was stirred in aqueous 1 M HCl solution (130 ml) at 70 °C for 6 hours in a capped round-bottomed flask. Mixture was allowed to cool down to ambient temperature and filtered. Solids were washed with distilled water (3 l). Washed solids were dried in an oven under air at 140 °C for 16 hours. Acid washed activated charcoal (4 g) was put into a lidless ceramic crucible and heated in an oven (heating ramp: 14 °C/min) under air for target time (usually 16 h) at target temperature (between 375 and 475 °C). Crucible was taken out of the oven after the oven had cooled to 68–81 °C (around 5 h) and was placed in a desiccator to cool to room temperature.

General procedure of carbocatalyzed 4-substituted quinolines synthesis. Carbon catalyst (17 mg, 100 mg/mmol of aniline) and a magnetic stirrer were placed in a 10 ml test tube, and stock solutions of target aniline (0.17 mmol, 1.15 equiv.), target aldehyde (0.15 mmol, 1 equiv.), and anisole (to reach 1.5 ml final volume) were added using automatic pipette. Atmosphere was changed to O_2 using 3 vacuum/O_2 cycles and the reaction flask was kept connected with the balloon during the reaction. The reaction was stirred at 140 °C for 6 h and cooled down to room temperature. The catalyst was filtered out on Celite and thoroughly washed with acetone (*ca.* 35 ml). The solvents were evaporated from the filtrate on rotary evaporator, and the crude was purified by subjecting it to flash chromatography on a silica gel.

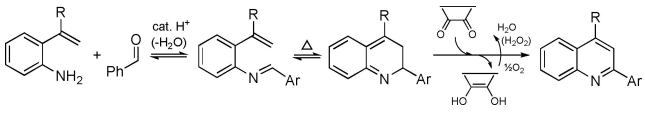

Scheme 3. Proposed reaction mechanism.

General procedure of carbocatalyzed 4-H-quinolines synthesis. Carbon catalyst (136 mg, 800 mg/mmol of aniline) and magnetic stirrer were placed in a 10 ml test tube equipped with conderser, and stirrer, stock solutions of target aldehyde (0.15 mmol, 1 equiv.), target aniline (0.17 mmol, 1.15 equiv.), and anisole (to reach 3 ml final volume) were added with an automatic pipettes. Atmosphere was changed to O_2 using 3 vacuum/O_2 cycles and kept connected to the flask during the reaction time. The reaction was refluxed at 170 °C for 40 h and cooled to room temperature. The catalyst was filtered out on Celite and thoroughly washed with acetone (*ca.* 35 ml). The solvents were evaporated from the filtrate on rotary evaporator, and the crude was purified by subjecting it to flash chromatography on a silica gel.

X-Ray diffraction studies

CCDC 2060091–2060096 contain the supplementary crystallographic data for compounds **4o**, **4q**, **4x**, **4ab**, **4ad**, and **4ae**. These data can be obtained free of charge from The Cambridge Crystallographic Data Centre via www.ccdc.cam.ac.uk/data_request/cif.

Acknowledgements

Financial support from Academy of Finland [project no. 129062 (J.H.)] is acknowledged. The Finnish National Centre for Scientific Computing (CSC) is recognized for computational resources.

References

[1] a) R. H. Manske, *Chem. Rev.* **1942**, *30*, 113–144; b) S. M. Prajapati, K. D. Patel, R. H. Vekariya, S. N. Panchal, H. D. Patel, *RSC Adv.* **2014**, *4*, 24463–24476; c) G. A. Ramann, B. J. Cowen, *Molecules* **2016**, *21*, 986–1009.

[2] V. Kouznetsov, L. Mendez, C. Gomez, *Curr. Org. Chem.* **2005**, *9*, 141–161.

[3] C. K. Chua, M. Pumera, *Chem. Eur. J.* **2015**, *21*, 12550–12562.

[4] a) M. Melchionna, S. Marchesan, M. Prato, P. Fornasiero, *Catal. Sci. Technol.* **2015**, *5*, 3859–3875; b) J. Figueiredo, M. F. R. Pereira *Carbon Materials for Catalysis. Carbon as Catalyst*, (Eds. P. Serp, J. L. Figueiredo), Wiley, **2008**.

[5] a) D. R. Dreyer, A. D. Todd, C. W. Bielawski, *Chem. Soc. Rev.* **2014**, *43*, 5288–5301; b) L. Lombardi, M. Bandini, *Angew. Chem. Int. Ed.* **2020**, *59*, 20767–20778; *Angew. Chem.* **2020**, *132*, 20951–20962.

[6] M. S. Ahmad, Y. Nishina, *Nanoscale* **2020**, *12*, 12210–12227.

[7] D. R. Dreyer, H.-P. Jia, C. W. Bielawski, *Angew. Chem. Int. Ed.* **2010**, *49*, 6813–6816; *Angew. Chem.* **2010**, *122*, 6965–6968.

[8] D. R. Dreyer, H.-P. Jia, A. D. Todd, J. Geng, C. W. Bielawski, *Org. Biomol. Chem.* **2011**, *9*, 7292–7295.

[9] S. Verma, H. P. Mungse, N. Kumar, S. Choudhary, S. L. Jain, B. Sain, O. P. Khatri, *Chem. Commun.* **2011**, *47*, 12673–12675.
[10] H.-P. Jia, D. R. Dreyer, C. W. Bielawski, *Adv. Synth. Catal.* **2011**, *353*, 528–532.
[11] Y. Gao, P. Tang, H. Zhou, W. Zhang, H. Yang, N. Yan, G. Hu, D. Mei, J. Wang, D. Ma, *Angew. Chem. Int. Ed.* **2016**, *55*, 3124–3128; *Angew. Chem.* **2016**, *128*, 3176–3180.
[12] K. Morioku, N. Morimoto, Y. Takeuchi, Y. Nishina, *Sci. Rep.* **2016**, *6*, 25824.
[13] H. Wu, C. Su, R. Tandiana, C. Liu, C. Qiu, Y. Bao, J. Wu, Y. Xu, J. Lu, D. Fan, K. P. Loh, *Angew. Chem. Int. Ed.* **2018**, *57*, 10848–10853; *Angew. Chem.* **2018**, *130*, 11014–11019.
[14] a) F. Hu, M. Patel, F. Luo, C. Flach, R. Mendelsohn, E. Garfunkel, H. He, M. Szostak, *J. Am. Chem. Soc.* **2015**, *137*, 14473–14480; b) L. Favaretto, J. An, M. Sambo, A. De Nisi, C. Bettini, M. Melucci, A. Kovtun, A. Liscio, V. Palermo, A. Bottoni, F. Zerbetto, M. Calvaresi, M. Bandini, *Org. Lett.* **2018**, *20*, 3705–3709.
[15] a) S. Verma, H. P. Mungse, N. Kumar, S. Choudhary, S. L. Jain, B. Sain, O. P. Khatri, *Commun. Chem.* **2019**, *2*, 113; b) H. Jung, C. W. Bielawski, *RSC Adv.* **2020**, *10*, 15598–15603.
[16] a) Y. Kawashita, N. Nakamichi, H. Kawabata, M. Hayashi, *Org. Lett.* **2003**, *5*, 3713–3715; b) N. Nakamichi, H. Kawabata, M. Hayashi, *J. Org. Chem.* **2003**, *68*, 8272–8273; c) T. Tanaka, K. Okunaga, M. Hayashi, *Tetrahedron Lett.* **2010** *51*, 4633–4635; d) M. Hayashi, *Chem. Rec.* **2008**, *8*, 252–267; e) Y. Kawashita, M. Hayashi, *Molecules* **2009**, *14*, 3073–3093; f) S. Kim, R. Matsubara, M. Hayashi, *J. Org. Chem.* **2019**, *84*, 2997–3003; g) Y. Kawashita, J. Yanagi, T. Fujii, M. Hayashi, *Bull. Chem. Soc. Jpn.* **2009**, *82*, 482–488.
[17] a) M. Krivec, M. Gazvoda, K. Kranjc, S. Polanc, M. Kočevar, *J. Org. Chem.* **2012**, *77*, 2857–2864; b) W. Yang, Y. Zhou, H. Sun, L. Zhang, F. Zhao, H. Liu, *RSC Adv.* **2014**, *4*, 15007–15010.
[18] a) J. E. Perea-Buceta, T. Wirtanen, O.-V. Laukkanen, M. K. Mäkelä, M. Nieger, M. Melchionna, N. Huittinen, J. A. Lopez-Sanchez, J. Helaja, *Angew. Chem. Int. Ed.* **2013**, *52*, 11835–11839; *Angew. Chem.* **2013**, *125*, 12051–12055; b) T. Wirtanen, M. K. Mäkelä, J. Sarfraz, P. Ihalainen, S. Hietala, M. Melchionna, J. Helaja, *Adv. Synth. Catal.* **2015**, *357*, 3718–3726; c) L. Enders, D. S. Casadio, S. Aikonen, A. Lenarda, T. Wirtanen, T. Hu, S. Hietala, L. S. Ribeiro, M. F. R. Pereira, J. Helaja, *Submitted manuscript*.
[19] a) D. R. Dreyer, C. W. Bielawski, *Chem. Sci.* **2011**, *2*, 1233; b) B. Wang, G. Wen, D. Su, *Nano Res.* **2017**, *10*, 2954–2965.
[20] J. López-Sanz, E. Pérez-Mayoral, E. Soriano, D. Omenat-Morán, C. J. Durán, R. M. Martín-Aranda, I. Matos, I. Fonseca, *ChemCatChem* **2013**, *5*, 3736–3742.
[21] a) S. Navalon, A. Dhakshinamoorthy, M. Alvaro, M. Antonietti, H. García, *Chem. Soc. Rev.* **2017**, *46*, 4501–4529; b) D. S. Su, G. Wen, S. Wu, F. Peng, R. Schlögl, *Angew. Chem. Int. Ed.* **2017**, *56*, 936–964; *Angew. Chem.* **2017**, *129*, 956–985.
[22] B. Daelemans, N. Bilbao, W. Dehaen, S. De Feyter, *Chem. Soc. Rev.* **2021**, *50*, 2280–2296.
[23] D. S. Casadio, S. Aikonen, A. Lenarda, M. Nieger, T. Hu, S. Taubert, D. Sundholm, M. Muuronen, T. Wirtanen, J. Helaja, *Chem. Eur. J.* **2021**, *27*, 5283–5291.
[24] M. R. Acocella, M. Mauro, L. Falivene, L. Cavallo, G. Guerra, *ACS Catal.* **2014**, *4*, 492–496.
[25] W. Qi, P. Yan, D. S. Su, *Acc. Chem. Res.* **2018**, *51*, 640–648.
[26] K. G. Qiang, N. H. Baine, *J. Org. Chem.* **1988**, *53*, 4218–4222.
[27] a) H. Walter, *J. Prakt. Chem.* **1998**, *340*, 309–314; b) X. Zhang, X. Xu, L. Yu, Q. Zhao, *Tetrahedron Lett.* **2014**, *55*, 2280–2282; c) S. W. Youn, J. H. Bihn, *Tetrahedron Lett.* **2009**, *50*, 4598–4601.
[28] F. P. Byrne, S. Jin, G. Paggiola, T. H. M. Petchey, J. H. Clark, T. J. Farmer, A. J. Hunt, C. Robert McElroy, J. Sherwood, *Sustain. Chem. Process.* **2016**, *4*, 7.
[29] T. Wirtanen, S. Aikonen, M. Muuronen, M. Melchionna, M. Kemell, F. Davodi, T. Kallio, T. Hu, J. Helaja, *Chem. Eur. J.* **2019**, *25*, 12288–12293.
[30] T. Wirtanen, M. Muuronen, J. Hurmalainen, H. M. Tuononen, M. Nieger, J. Helaja, *Org. Chem. Front.* **2016**, *3*, 1738–1745.